Electronic properties and optical spectra of MoS_2 and WS_2 nanotubes

Ivanka Milošević,* Božidar Nikolić, Edib Dobardžić, and Milan Damnjanović
NanoLab, Faculty of Physics, University of Belgrade, P.O. Box 368, 11001 Belgrade, Serbia

Igor Popov and Gotthard Seifert
Physikalische Chemie, TU Dresden, D-01062 Dresden, Germany
(Received 24 August 2007; published 28 December 2007)

Symmetry based calculations of the polarized optical absorption in single-wall MoS_2 and WS_2 nanotubes are presented. Optical conductivity tensor for the individual tubes, using line group symmetry and density-functional tight binding implemented in POLSYM code, is numerically evaluated and its dependence on the diameter and chiral angle of the nanotubes is investigated. This minimal, full symmetry implementing algorithm enabled calculations of the optical response functions very efficiently and addressed the large diameter tubes and highly chiral tubes as well. It is predicted that, due to the symmetry transformation properties of the relevant electronic states, fluorescence is not expected in the metal dichalcogenide tubes. In accordance with the measurements, the calculations show redshift of the absorption peaks as the tube diameter increases. Also, it is found that curvature strain induces strong chiral angle dependence of the absorption spectra.

DOI: 10.1103/PhysRevB.76.233414 PACS number(s): 78.67.Ch, 61.46.Fg, 73.22.−f

The first report on synthesis of transition metal dichalcogenide nanotubes by Tenne *et al.*[1] triggered extensive research of the inorganic nanostructures which proved to have potential of becoming a key nanotechnological material due to the outstanding physical properties.[2,3] Optical absorption[4,5] and Raman spectra measurements[5,6] of the MS_2 (M=Mo,W) nanostructures were reported in the late 1990s. Shortly after, the electronic band calculations were carried out by the density-functional tight-binding (DFTB) method.[7,8] Experimental and theoretical studies on single MS_2 nanotubes, phonon dispersion calculations,[9] and resonance Raman scattering[10,11] have been reported quite recently. The optical response functions, however, have not been evaluated thus far.

In this Brief Report, we present symmetry based calculations of the polarized optical absorption of MS_2 nanotubes. We evaluate numerically the optical conductivity tensor for the individual tubes using line group symmetry implemented in the POLSYM code[12] and DFTB based wave functions.[13] This minimal, full symmetry implemented algorithm enables us to evaluate optical response functions very efficiently and to consider the highly chiral tubes (which have a huge number of atoms within a unit cell) as well. Namely, instead of the unit cell, the *symcell*[14] (i.e., the minimal set of atoms from which, by applying *all* symmetry transformations, the whole tube can be generated) is used. As the symcell of a single-wall MS_2 nanotube (NT) contains three atoms[15] (irrespective of the chirality of the tube) while the number of atoms within the unit cell may be extremely large, tremendous computation-time savings are achieved enabling us to perform calculations on the large set of MS_2 tubes of different types: from the narrow nanotubes to the (a)chiral microtubes.

Single-wall MS_2 tube can be imagined as a single MS_2 layer with trigonal prismatic coordination[16] rolled up into a cylinder: sulfur shells are symmetrically arranged with respect to the metal one. The chiral vector (n_1,n_2) is defined within the metal plane. Symmetry groups of the chiral (n_1,n_2), $n_1>n_2$, zigzag $(n,0)$, and armchair (n,n) nanotubes are described by the line groups[15] (parameters of which are fully determined by chiral indices).

Unlike the case of carbon nanotubes, zigzag and armchair tubes of MS_2 kind differ in symmetry: mirror planes are vertical (containing the tube axis) in the former and horizontal (perpendicular onto the tube axis) in the latter. Therefore, in addition to linear and angular quasimomenta quantum numbers (k and m), there are parities related to the vertical and horizontal mirror planes.

However, the described rolled-up layer configuration is not the equilibrium one, as the curvature induces an additional tension with respect to the layer. Therefore, in order to find the stable configurations, symmetry preserving optimization of the structure within the DFTB approach was performed. As, according to the topological theorem of Abud and Sartori,[17] the extremes of the invariant functions are on the manifolds with maximal symmetry, apart from the translational unit, only the coordinates of the symcell atoms are varied.

The relaxation procedure showed that the stable configuration of the tubes with diameters between 6 and 20 nm can be obtained by rolling up a somewhat stretched MS_2 layer (lattice constant change within the S and M atomic planes is 0.25 Å, while the stretching of the inner and outer $M-S$ bonds are 0.01 and 0.04 Å, respectively). For the thick tubes ($D>20$ nm), the relaxation effects were negligible, while for the narrow tubes ($D<6$ nm), full relaxation had to be performed.

Electronic band calculations are performed within the DFTB approach. From each atom, only the valence shell orbitals are considered. In particular, for sulfur, one $3s$ and three $3p$, while for molybdenum and tungsten, the outer s, p, and d atomic orbitals are used. The structures were optimized, i.e., within the DFTB approach, all chirality dependent distortions of the nanotube structures are taken into account.

Electron band structure calculations of large systems with

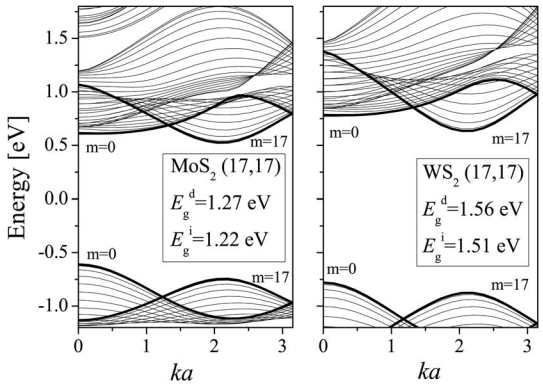

FIG. 1. Electronic bands in the Fermi level region of the (17,17) MS_2 NTs. The gap sizes are shown in the insets.

high symmetry are most efficiently carried out with the help of modified Wigner projectors.[14] Namely, this formalism requires only the orbit representative atoms, the symcell atoms, to be taken into account, which, in highly symmetric systems, tremendously reduces the order of the secular equation. In particular, whatever the chirality of the considered MS_2 NT is, only the space spanned by the relevant orbitals from the three atoms is sufficient for calculation.

The energy bands obtained are labeled by a complete set of quantum numbers: k (quasimomentum) taking on values from the interval $(-\pi/a, \pi/a]$ and m (z component of the angular momentum) taking on integer values from the interval $(-q/2, q/2]$, where q is determined by n_1 and n_2 (details are given in Ref. 15). In the cases of the zigzag and armchair tubes, there are additional parities related to the vertical and horizontal mirror planes (even/odd denoted by A/B and $\pm$), respectively, leading to the reductions of the quantum numbers' domains ($m \in [0, q/2]$ for the armchair and $k \in [0, \pi/a]$ for the zigzag tubes) reflecting itself in the double band degeneracies in the interior of the domains unlike the nondegenerated chiral tubes' bands. This is illustrated in Figs. 1 and 2, where the band structure around the Fermi energy of (17,17) and (30,0) MS_2 tubes is given. The diameter of the tubes is ~3 nm while their unit lengths differ considerably. The size of the band gaps of these tubes does not differ much, but the band gaps are of different types:

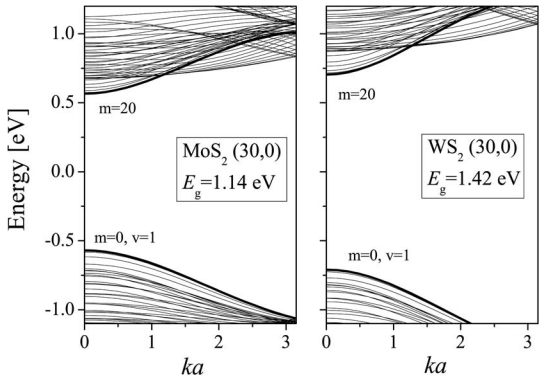

FIG. 2. Electronic bands in the Fermi level region of the (30,0) MS_2 NTs. The gap sizes are shown in the insets.

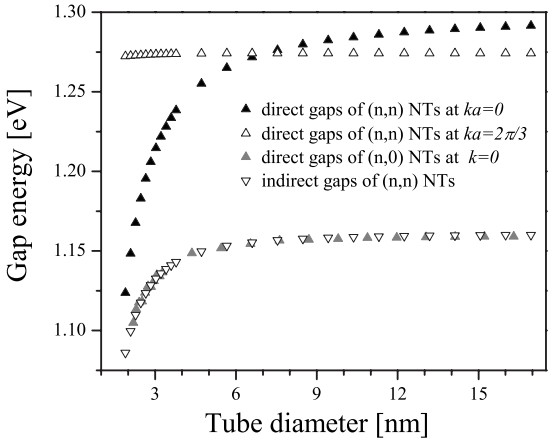

FIG. 3. Calculated gap energies E of the achiral MoS_2 NTs as a function of the tube diameter D.

(30,0) NTs have a direct gap at $ka=0$, while (17,17) NTs have an indirect gap (maximum of the highest valence band is at $ka=0$ and minimum of the lowest conducting band is at $ka=2\pi/3$).

The band gaps for the achiral MoS_2 and WS_2 NTs with diameters from 2 to 17 nm are systematically investigated and the results are presented in Figs. 3 and 4. Both molybdenum and tungsten disulfide armchair NTs have a small indirect gap ($0 \rightarrow 2\pi/3$), which is similar to the direct gap (at $ka=0$) of the corresponding zigzag NTs. Besides the indirect gap (which is small in the case of the MoS_2 and moderate in the case of the WS_2 NTs), the armchair MS_2 NTs exhibit moderate direct gaps at $ka=0$ and at $ka=2\pi/3$. The size of the latter is almost independent of the diameter: ~1.27 eV (MoS_2 NTs) and ~1.5 eV (WS_2 NTs), slightly exceeding the indirect gap values of the corresponding $2H$ bulk materials.

On the other hand, the value of the direct gap at $ka=0$ increases with the diameter and exceeds the direct gap at $ka=2\pi/3$ if the diameter of the MoS_2 (WS_2) NT becomes larger than 7.5 nm (2.5 nm). The gap structure of the molybdenum and tungsten disulfide achiral tubes is quite similar. Roughly, the D dependence of the gap sizes of the WS_2 NTs

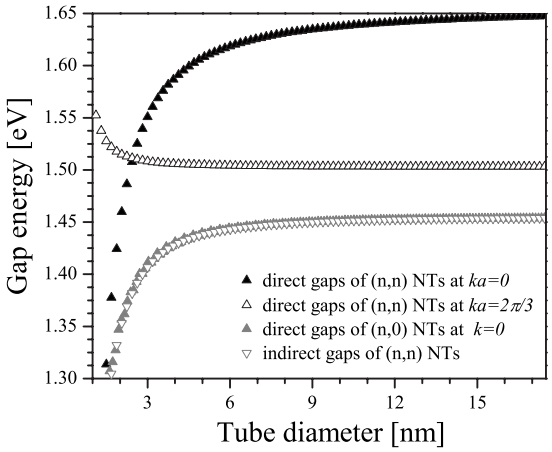

FIG. 4. Calculated gap energies E of the achiral WS_2 NTs as a function of the tube diameter D.

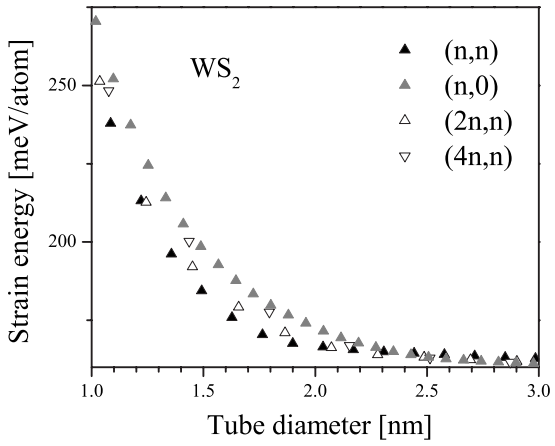

FIG. 5. Curvature induced strain energy of WS_2 NTs as a function of the tube diameter.

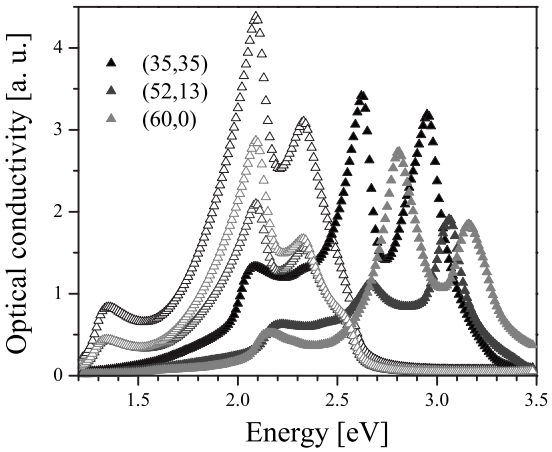

FIG. 6. Optical conductivity of the (35,35), (52,13), and (60,0) MoS_2 NTs. Open symbols show calculated spectra of the corresponding unrelaxed (i.e., simply rolled up from a single MoS_2 layer along the chiral vector) nanotubes.

can be obtained by simply, upshifting the corresponding MoS_2 gaps for ~250 meV.

Optical transitions between the bands which form the direct band gaps in the MS_2 armchair tubes are allowed as they have the same quasiangular momentum m quantum numbers: $m=0$ and $m=n$ for the bands forming direct gaps at $ka=0$ and $ka=2\pi/3$, Fig. 1. However, the direct gap in the zigzag tubes cannot be seen in the optical absorption spectra as the corresponding bands are characterized by different quantum numbers m. For instance, in the case of (30,0) MS_2 NTs (at $ka=0$), the uppermost valence band has zero quasiangular momentum quantum number, while the lowest conducting band is characterized by $m=20$ (Fig. 2). Thus, in contrast to carbon nanotubes,[18] the structured band gap photoluminescence (fluorescence) is not expected here.

In Fig. 5, the calculated diameter dependencies of the curvature strain energies of WS_2 NTs, i.e., the differences of the total energies (per atom) between the tube and the layer, are shown. It roughly follows a $1/D^2$ behavior as in molybdenum disulfide[7] and carbon[19] NTs. The armchair WS_2 NTs are found to be more stable than the zigzag ones, while the other chiralities interpolate well the two boundaries. Unlike the unrelaxed configuration which assumes the bond lengths and bond angles to be unchanged, the optimized MS_2 NTs exhibit chirality dependence of the optical absorption spectra, Fig. 6.

The optical response of the MS_2 NTs is obtained by means of first-order time dependent perturbation theory. The real part of the polarized optical conductivity is evaluated within the dipole approximation and the optical transition matrix elements are calculated out of the completely symmetry adapted Bloch eigenfunctions.[21] Details of the method can be found in Ref. 20. The only difference is that in this Brief Report, we deal with a three orbit system and larger number of the valence shell orbitals.

The so-called antenna effect, which has been predicted and confirmed for carbon nanotubes,[22] is manifested also in the single-wall MS_2 NTs. The calculated optical spectra show highly anisotropic absorption. Optical response is present only for polarization parallel to the tube axis. Besides, the ratio of the perpendicular and parallel polarizability tensor components estimated from the resonant Raman scattering measurements[11] on individual WS_2 NTs is not larger than 0.16. Hence, as the depolarization effect strongly suppresses light polarized perpendicular to the nanotube axis, we consider only the absorption of the parallely polarized light.

In Fig. 6, typical optical conductivity spectra (in the visible region) of the MoS_2 NTs with the same diameters (D ~6.1 nm) but different chiralities are given. In order to estimate the effect of the curvature strain, the spectra of the corresponding unrelaxed tubes (i.e., simply rolled up from a single layer) are also shown. The latter exhibits no chiral sensitivity whatsoever, unlike the spectra of the optimized tubular structures. Namely, the curvature strain induces chirality dependence of the absorption spectra and shifts the absorption peaks toward higher energies. Such a property can be exploited in various sensoric applications. The same holds for WS_2 tubes; only their absorption peaks are somewhat blueshifted relative to the MoS_2 NTs' spectra, as shown in Fig. 7. Finally, as can be seen by comparing Figs. 6 and 7,

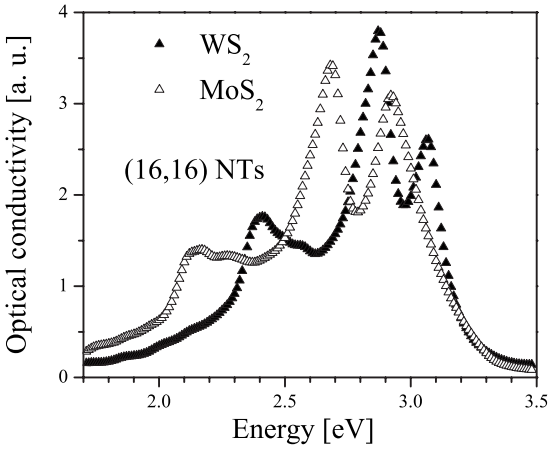

FIG. 7. Optical conductivity of the (16,16) MoS_2 and WS_2 NTs.

there is a redshift of the absorption peaks as the tube diameter increases, in accordance with the previous experimental measurements.[4–6]

In conclusion, using a very efficient methodology, electro-optical properties of a quite large sample of single-wall MS_2 NTs (including the highly chiral ones) have been calculated. Diameter and chirality dependences of the electronic band gaps and optical spectra features are investigated and MS_2 NTs are found to possess interesting and unique optical characteristics, assuring predictable and well-controllable optical properties of the future, MS_2 NT-based nano-optoelectronic devices.

This work is supported by the Serbian Ministry of Science (Project No. ON141017) and European Union (FP6 INCO-WBC 026303 project).

*ivag@rcub.bg.ac.yu

[1] R. Tenne, L. Margulis, M. Genut, and G. Hodes, Nature (London) **360**, 444 (1992).
[2] R. Tenne, M. Homyonfer, and Y. Feldman, Chem. Mater. **10**, 3225 (1998).
[3] M. Remškar, Adv. Mater. (Weinheim, Ger.) **16**, 1 (2004).
[4] G. L. Frey, S. Elani, M. Homyonfer, Y. Feldman, and R. Tenne, Phys. Rev. B **57**, 6666 (1998).
[5] G. L. Frey, R. Tenne, M. J. Matthews, M. S. Dresselhaus, and G. Dresselhaus, J. Mater. Res. **13**, 2412 (1998).
[6] G. L. Frey, R. Tenne, M. J. Matthews, M. S. Dresselhaus, and G. Dresselhaus, Phys. Rev. B **60**, 2883 (1999).
[7] G. Seifert, H. Terrones, M. Terrones, G. Jungnickel, and T. Frauenheim, Phys. Rev. Lett. **85**, 146 (2000).
[8] G. Seifert, H. Terrones, M. Terrones, G. Jungnickel, and T. Frauenheim, Solid State Commun. **114**, 245 (2000).
[9] E. Dobardžić, B. Dakić, M. Damnjanović, and I. Milošević, Phys. Rev. B **71**, 121405(R) (2005); E. Dobardžić, I. Milošević, B. Dakić, and M. Damnjanović, *ibid.* **74**, 033403 (2006).
[10] M. Viršek, A. Jisih, I. Milošević, M. Damnjanović, and M. Remškar, Surf. Sci. **601**, 2868 (2007).
[11] P. M. Rafailov, C. Thomsen, K. Gartsman, I. Kaplan-Ashiri, and R. Tenne, Phys. Rev. B **72**, 205436 (2005).
[12] I. Milošević, A. Damjanović, and M. Damnjanović, in *Quantum Mechanical Simulation Methods in Studying Biological Systems*, edited by D. Bicout and M. Field (Springer-Verlag, Berlin 1996) Chap. XIV.
[13] D. Porezag, T. Frauenheim, T. Köhler, G. Seifert, and R. Kaschner, Phys. Rev. B **51**, 12947 (1995).
[14] M. Damnjanović, I. Milošević, E. Dobardžić, T. Vuković, and B. Nikolić, in *Applied Physics of Nanotubes: Fundamentals of Theory, Optics and Transport Devices*, edited by S. V. Rotkin and S. Subramoney (Springer-Verlag, Berlin, 2005), pp. 41–88.
[15] I. Milošević, T. Vuković, M. Damnjanović, and B. Nikolić, Eur. Phys. J. B **17**, 707 (2000).
[16] *Structrual Chemistry of Layer-Type Phases*, edited by F. Lévy (Reidel, Dordrecht, 1976).
[17] H. Abud and G. Sartori, Ann. Phys. (N.Y.) **150**, 307 (1983).
[18] R. B. Weisman, S. M. Bachilo, and D. Tsyboulski, Appl. Phys. A: Mater. Sci. Process. **78**, 1111 (2004).
[19] E. Hernández, C. Goze, P. Bernier, and A. Rubio, Phys. Rev. Lett. **80**, 4502 (1998).
[20] I. Milošević, T. Vuković, S. Dmitrović, and M. Damnjanović, Phys. Rev. B **67**, 165418 (2003).
[21] I. Milošević, B. Dakić, and M. Damnjanović, J. Phys. A **39**, 11833 (2006).
[22] H. Ajiki and T. Ando, J. Phys. Soc. Jpn. **62**, 4267 (1993).